Position sensitivity of graphene field effect transistors to X-rays

Edward Cazalas, Biddut K. Sarker, Michael E. Moore, Isaac Childres, Yong P. Chen, and Igor Jovanovic

---

Articles you may be interested in

Graphene nanopore field effect transistors
J. Appl. Phys. **116**, 023709 (2014); 10.1063/1.4889755

Substrate dielectric effects on graphene field effect transistors
J. Appl. Phys. **115**, 194507 (2014); 10.1063/1.4879236

Linearity of graphene field-effect transistors
Appl. Phys. Lett. **103**, 173115 (2013); 10.1063/1.4826932

Influence of metal work function on the position of the Dirac point of graphene field-effect transistors
Appl. Phys. Lett. **95**, 243105 (2009); 10.1063/1.3274039

X-ray-induced recombination effects in a-Se-based x-ray photoconductors used in direct conversion x-ray sensors
J. Vac. Sci. Technol. A **22**, 1005 (2004); 10.1116/1.1701856

Position sensitivity of graphene field effect transistors to X-rays

Edward Cazalas,[1,a),b)] Biddut K. Sarker,[2,3,b)] Michael E. Moore,[1] Isaac Childres,[2,3] Yong P. Chen,[2,3,4] and Igor Jovanovic[1]

[1]*Department of Mechanical and Nuclear Engineering, The Pennsylvania State University, University Park, Pennsylvania 16802, USA*
[2]*Department of Physics and Astronomy, Purdue University, West Lafayette, Indiana 47907, USA*
[3]*Birck Nanotechnology Center, Purdue University, West Lafayette, Indiana 47907, USA*
[4]*School of Electrical and Computer Engineering, Purdue University, West Lafayette, Indiana 47907, USA*

Device architectures that incorporate graphene to realize detection of electromagnetic radiation typically utilize the direct absorbance of radiation by graphene. This limits their effective area to the size of the graphene and their applicability to lower-energy, less penetrating forms of radiation. In contrast, graphene-based transistor architectures that utilize the field effect as the detection mechanism can be sensitive to interactions of radiation not only with graphene but also with the surrounding substrate. Here, we report the study of the position sensitivity and response of a graphene-based field effect transistor (GFET) to penetrating, well-collimated radiation (micro-beam X-rays), producing ionization in the substrate primarily away from graphene. It is found that responsivity and response speed are strongly dependent on the X-ray beam distance from graphene and the gate voltage applied to the GFET. To develop an understanding of the spatially dependent response, a model is developed that incorporates the volumetric charge generation, transport, and recombination. The model is in good agreement with the observed spatial response characteristics of the GFET and predicts a greater response potential of the GFET to radiation interacting near its surface. The study undertaken provides the necessary insight into the volumetric nature of the GFET response, essential for development of GFET-based detectors for more penetrating forms of ionizing radiation. © 2015 AIP Publishing LLC. [http://dx.doi.org/10.1063/1.4921755]

Graphene's unique electrical properties make it a promising material for detection architectures. In this context, there has been intense interest and research activity in graphene-based transistors, which have been found to offer high speed, broad spectral range, and high sensitivity.[1–4] Those characteristics indicate the potential of graphene-based device architectures to provide important advances to electronic and sensing technologies.[5–7]

Various graphene-based detectors have been investigated, with an aim to enhance the responsivity and to understand the physical mechanism of response.[8–11] In past work, graphene-based detectors have shown response to THz, infrared, visible, and UV light, but the mechanism of detection was based on direct interaction with the graphene, which absorbs only a small fraction of incident radiation.[11–16] The utilization of graphene for X-ray detection has been limited to several recent studies.[17–19]

Here, we investigate the performance of a graphene-based field effect transistor (GFET), a graphene-based detector designed to perform detection by means of interaction with the device substrate instead of direct interaction with the graphene. GFET is a relatively simple transistor architecture that is constructed by placing the graphene onto a back-gated semiconductor substrate, as shown in Figure 1(a). Unlike other graphene-based detectors, which rely on direct interaction of radiation with graphene[14–16,20–23] or a quantum

dot layer adjacent to graphene,[11,24] the GFET architecture may be operated as a relatively large-area, large-volume radiation detector by exploiting the field effect principle. In this approach, the field effect refers to the modulation of graphene charge carrier density by changes in local electric field experienced by graphene. Such changes in electric field may be induced by production and transport of electron-hole pairs within the substrate when exposed to radiation. In this detection architecture, the measured property of a GFET that indicates the interaction with the radiation field is the conductivity change of graphene, which depends on the rate and extent of energy deposition, substrate electrical characteristics, and the gate voltage applied to the GFET.[25–28]

The objective of this work is to develop an understanding of the sensitivity of GFETs to X-ray energy deposition occurring away from graphene. This is achieved by studying the GFET response to a highly penetrating, focused X-ray microbeam, which is positioned at lateral points across the GFET. The use of X-rays allows the fairly uniform generation of electron-hole pairs throughout the depth of the substrate, enabling the study of GFET sensitivity to radiation energy deposition in both the lateral dimension and over an integrated range of depths, as shown in Figure 1(b). Various other operational characteristics of the GFETs have been studied to date, including the potential for field effect response,[25,28–30] hysteretic effects,[31–34] and the dependence of GFET response to various radiation types and energies.[17,18,35–37] Our particular interest is in evaluating the potential for development of position sensitive GFETs, and GFETs that employ small-area graphene yet are

---

a)Author to whom correspondence should be addressed. Electronic mail: ejc149@psu.edu
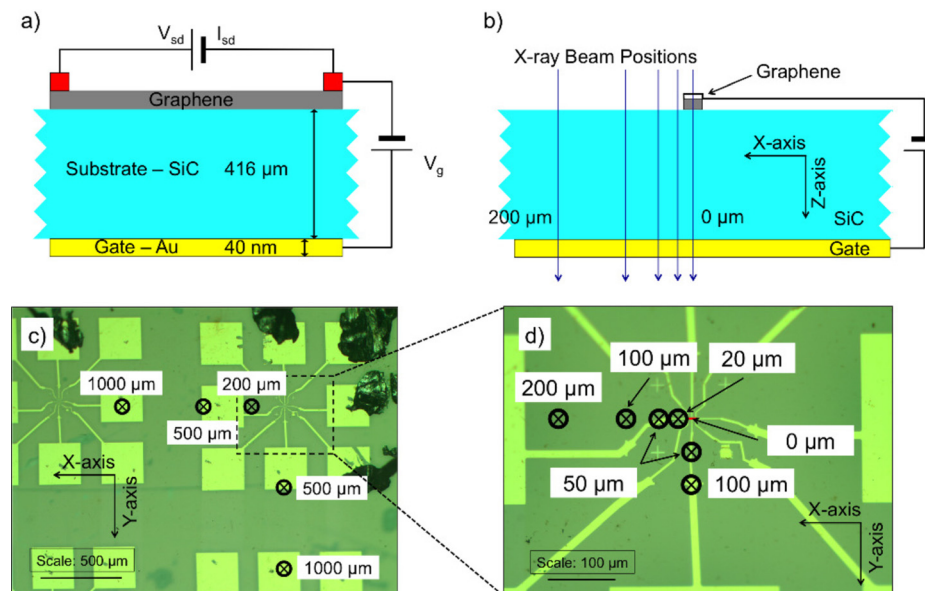b)E. Cazalas and B. K. Sarker contributed equally to this work.

FIG. 1. (a) The GFET device structure comprises of the graphene on an electrically gated, undoped SiC substrate. Electrical contacts are used to provide the gate voltage (V_g) and the source-drain voltage (V_{sd}), and enable the measurements of graphene current (I_{sd}). (b) The experiment is conducted by exposing the GFET to an X-ray beam at several positions along both transverse axes (distances are measured from the center of graphene). The X-ray beam penetrates through the substrate along the Z-axis (depth into the substrate). (c) The top surface of the GFET is shown, and the device used for the experiment is located in the upper right corner of the figure. The square gold pads are used for wire-bonding. Positions of X-ray beam exposure are shown as circled crosses ($\otimes$) in the X-axis (horizontal) and Y-axis (vertical), along with the distance from the center of graphene. (d) A magnified view of the GFET surface within the dotted box in c) is displayed.

sensitive to radiation over much larger device areas. It is also important that the devices be sensitive to energetic, highly penetrating radiation, to support a number of important radiation detection applications which require a combination of high-resolution and spatially dependent charge deposition measurements.[38–40] To address those needs, we performed an experiment utilizing an X-ray microbeam facility provided by the Advanced Photon Source at Argonne National Laboratory. The results offer insight into the position-dependent response of GFETs to high-energy (>keV) photon irradiation.

We identify three desirable characteristics of a photon probe needed for high-fidelity position-sensitive measurements of the GFET response. First, measurements of the transverse (lateral) dimension require a beam with diameter no greater than several μm, such that it is significantly smaller than the size of graphene in the GFET device. Second, high-energy photons (X-rays) in the multi-keV beam can effectively penetrate the thickness of the substrate and contribute to the response not only from ionization near the device surface, but all along the depth of the X-ray beam through the substrate. Finally, the use of a monoenergetic X-ray beam with low energy spread allows high confidence in the energy deposition profile produced in the experiment. The 34-ID-E undulator beamline of the Advanced Photon Source at Argonne National Laboratory produces X-rays with those characteristics and also provides a high X-ray rate (approximately $4.2 \times 10^9 \, \gamma/\text{s}$ during the course of the experiment). The 34-ID-E beamline has a beam size of $\approx 0.3 \times 0.3 \, \mu\text{m}^2$ and produces monoenergetic $\text{E} = 15 \, \text{keV}$ X-rays with a relative energy spread $\Delta E/E \approx 1 \times 10^{-4}$. While lattice damage and defects are expected to be created in SiC due to the intense beam of radiation, it is estimated that the dose to the substrate volume (approximately up to 1

kGy) is insufficient to significantly affect device performance as it has been shown in prior work that the changes in SiC I–V characteristics, leakage current, and charge collection occur at much greater doses (greater than 20 kGy).[41,42] While these previous studies do not directly investigate GFETs, the relevant electronic properties investigated as a function of dose are similarly affected in our devices due to the requirement for excess charge generation and transport in the SiC substrate.

The X-ray beam was focused at different positions on the device, ranging from the center of graphene to 1000 μm away from graphene in both lateral axes. The locations of those positions in relation to the other device features are shown in Figures 1(c) and 1(d). The dimension of graphene is approximately $20 \times 4 \, \mu\text{m}^2$ and was determined to be monolayer using Raman spectroscopy (see Section I in the supplementary material for method of GFET fabrication and measurement[54]). $I_{sd} - V_g$ measurements (where I_{sd} is graphene source-drain current and V_g is gate voltage) show a clear unipolar field-effect response of the graphene during the X-ray beam exposure when compared to the absence of X-ray exposure (see Supplementary Figure S1[54]). When the X-ray beam is incident at locations closer to the graphene, the field effect increases in magnitude. When the X-ray beam is incident onto the top surface of the GFET, it occasionally passes through gold contacts or pads on the device surface. However, this was determined not to measurably affect the GFET response (see Section III in the supplementary material III[54]).

Time-dependent measurements, $I_{sd} - t$, have also been conducted by shuttering the X-ray beam. $I_{sd} - t$ responses at several X-ray beam positions are shown for X- and Y-axis in Figures 2(a) and 2(b), respectively. During the course of those measurements, the applied gate voltage remained
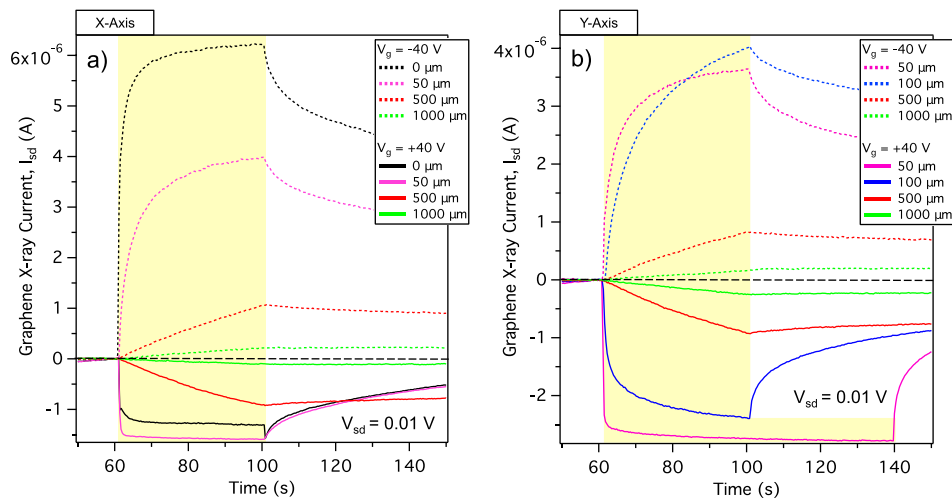
FIG. 2. (a) $I_{sd} - t$ when substrate is exposed to X-ray beam (yellow shaded regions) for positions in the *X*-axis, and (b) *Y*-axis. The exposures have durations of ~40 s (60–100 s), with a recovery period of ~80 s (100–150 s). An exception is in (b), where for $Y = 50\,\mu$m, the exposure occurs during 60–140 s. During each measurement, gate voltage is constant with $V_g = -40$ V (positive current response) and $+40$ V (negative current response). The dashed black line at $I_{sd} = 0$ A represents the absence of exposure, when only the dark current is measured (typical dark current is ~10 μA). The dark current subtracted from each $I_{sd} - t$ measurement is the graphene current measured at time $t = 55$ s (before the X-ray irradiation).

constant at $V_g = -40$ V or $+40$ V. Time-dependent graphene response is consistent with $I_{sd} - V_g$ measurements both in magnitude and direction of conductivity change.

From the time dependence measurements shown in Figure 2, the responsivity, $\Delta I_{sd}/P_{inc}$ (where $P_{inc} = 10.1\,\mu$W is the incident X-ray power, see Section IV in the supplementary material IV for the calculation of power[54]), and the time constant, τ, of the response are extracted, as given in Figs. 3(a) and 3(b), respectively. Time constant is measured for the initial response to X-ray irradiation. Responsivity at each position is calculated by determining the change in graphene current, ΔI_{sd}, due to X-ray beam exposure, as shown in Figure 2. In Figures 3(a) and 3(b), the data from all measurement positions (including those not shown in Figure 2) are reported.

As the X-ray beam is translated far (more than ~100 μm) away from graphene, the GFET responsivity in Figure 3(a) shows a rapid decrease, while the time constant in Figure 3(b) shows a rapid increase. The drop in responsivity shows that the effect of ionization on the electric field near graphene is reduced when the location of ionization is at a greater distance from graphene, suggesting a reduced efficiency of the transport of electrons (for negative back gate voltages) or holes (for positive back gate voltages) to

graphene. Reduced charge carrier transport efficiency to graphene results from the increased probability of carrier capture by substrate defects and impurities, or recombination with charge carriers of opposite sign, as the distance over which the carriers are transported increases. The maximum responsivity obtained with our GFET in the X-ray measurements is $R = 0.62$ A/W for $V_g = -40$ V with X-ray beam position centered on graphene ($X = 0\,\mu$m). This responsivity is greater than that of established X-ray detectors.[43–45] Further information regarding the calculation of responsivity and time constant is supplied in Section IV of the supplementary material.[54]

For irradiation occurring less than 20–50 μm from graphene, the relatively small change in responsivity indicates a saturation effect, whereby the conductivity of graphene is no longer very sensitive to changes in the X-ray beam exposure position. The saturation is clearly observed in Figure 2 and is dependent on gate voltage polarity and magnitude (details of gate voltage dependence are given in Section V of the supplementary material[54]), as higher saturation levels are observed for negative gate voltage, $V_g = -40$ V. This indicates that the saturation may be dependent on the charge carrier type being transported toward graphene (electrons for negative gate voltage, which have approximately an order of
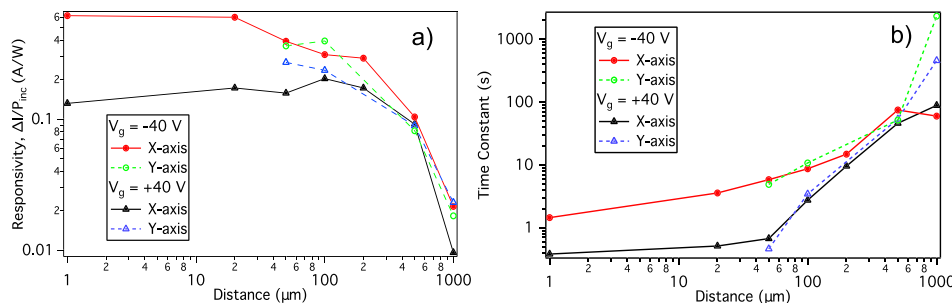

FIG. 3. (a) Responsivity to incident X-ray beam power, $\Delta I_{sd}/P_{inc}$ at various *X* (solid lines and filled markers) and *Y* (dotted lines and unfilled markers) positions of the X-ray microbeam for $V_g = -40$ V (circle markers) and $+40$ V (triangle markers). (b) The time constant of graphene response to X-ray beam exposure for various positions of the microbeam in the *X*-axis (solid lines and filled markers) and *Y*-axis (dotted lines and unfilled markers) for $V_g = -40$ V (circle markers) and $V_g = +40$ V (triangle markers).

magnitude higher mobility than holes)[46] in the substrate. The negative spike observed for $V_g = 40$ V and $X = 0$ μm at $t = 100$ s is believed to be due to the switching of charge carrier type in graphene, where the changes in the electric field near graphene are sufficiently large to overcome the preexisting p-type doping of the graphene.[31,33,47] The time constant of GFET response observed in this work is much greater than the time constant of established X-ray detectors (of order of ns–ps).[48–50] One mechanism that can cause the slow response time and variations in graphene current studied previously is electrochemical doping.[31] Long-term exposure of the device to ambient air, including humidity, induces electrochemical doping of the device, which has been shown to affect speed, stability of response, and reproducibility of field effect measurements in other carbon nanotube and graphene-based devices.[51–53] Further information about mechanisms and repeatability of GFET response is provided in Section VI of the supplementary material.[54] Future practical devices will require a significant reduction of electrochemical doping both through the fabrication process and isolation of graphene from the surrounding environment (for example, by sealing the device).

A model was developed to aid in the understanding of mechanism(s) that lead to graphene response to X-ray beam exposure and to assess the responsivity of the GFET as a function of lateral position and depth of radiation energy deposition. The model assumes: (1) Graphene current is modulated when the ionization-produced charge carriers in the SiC substrate are transported to the vicinity of graphene (immediately beneath graphene); (2) the graphene response is nonlinearly dependent on the number of charge carriers in the vicinity of graphene; (3) during the charge carrier transport, a fraction of them become trapped at defect and impurity sites and eventually recombine with their opposite charges, thus not contributing to GFET response; (4) an equilibrium is achieved during which the number of generated charge carriers transported toward graphene is equal to the number being captured and subsequently recombined. The model calculations are performed considering the transport of a sample charge from an array of locations (lateral position and depth) within the substrate. Further analytical description of the model is provided in Section VII of the supplementary material.[54] The model is fitted to the measured graphene responsivity, as in Figure 4(a). Once the fitting parameters are obtained (also discussed in detail in

Section VII of the supplementary material[54]), they are reapplied to the model to predict the responsivity of the GFET as a function of lateral position (X- and Y-axis) and depth (Z-axis). This charge transport efficiency (transport factor, T) map, shown in Figure 4(b), may be used to predict GFET responsivity due to radiation interaction at a position or range of positions within the GFET, given the fitted nonlinearity of graphene response, α (see Supplementary Table 1 for fitted α values[54]). The model generally shows decreasing charge transport efficiency as a function of increasing distance from graphene, equidistant from graphene.

In summary, the spatially dependent response characteristics of a GFET to X-ray radiation were studied by use of a microbeam X-ray facility (34-ID-E beamline of the Advanced Photon Source at Argonne National Laboratory). Time-dependent graphene current measurements were conducted during GFET irradiation at various lateral positions on the GFET with monochromatic X-rays at an energy $E_\gamma = 15$ keV and with the GFET biased under constant gate voltage. From these time-dependent measurements, responsivity and speed of GFET response were extracted. Results show a maximum responsivity of $R = 0.62$ A/W ($V_g = -40$ V) when the X-ray beam passes through the center of graphene. The responsivity drops rapidly with the increase in distance of X-ray irradiation position far away from graphene, while the speed of response (measured by the time constant τ) is also reduced. As expected, no significant differences in responsivity or time constant were observed for equal positions in the X- and Y-axis. However, the gate voltage has been found to affect the GFET response to X-rays. Higher responsivities and shorter response time constants have been measured for negative gate voltages, likely due to the difference between electron and hole mobility in the SiC substrate and/or electrochemical effects. A model for the GFET response has been developed and utilized to gain understanding into the interplay of the mechanisms affecting the spatially-dependent GFET response, including carrier generation by the X-rays, their transport, and recombination in the substrate. The model predicts the nearly equal charge transport efficiency in all dimensions for equal distance from the graphene. The GFET we have fabricated, tested, and characterized shows a strong position dependence and responsivity greater than that of established X-ray detectors, which is attributed to a different detection mechanism, which in our case employs the field effect. The study performed
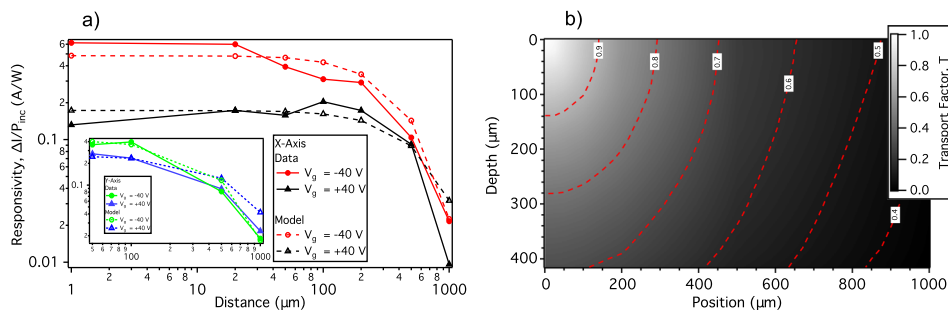

FIG. 4. (a) The fit of the model (dashed lines, unfilled markers) to experimental data of graphene responsivity (solid lines, filled markers) is given for X- and Y-axis (inset). The model is fitted to the X-axis data using least square regression. (b) The charge transport efficiency (transport factor, T) of the GFET as a function of lateral position (X- or Y-axis) and depth (Z-axis) in the substrate is mapped with graphene located at Position=Depth=0 μm (upper left). The calculated quantity is the fraction of generated charge carriers that are transported to the location in the substrate immediately below graphene.

herein enhances the understanding of the GFET response to penetrating ionizing radiation and provides groundwork for the development of GFET radiation sensors with position sensitive, high-energy photon and charged particle detection applications.

[1]G. Moddel, Z. Zhu, S. Grover, and S. Joshi, Solid State Commun. **152**, 1842 (2012).

[2]M. Mittendorff, S. Winnerl, J. Kamann, J. Eroms, D. Weiss, H. Schneider, and M. Helm, Appl. Phys. Lett. **103**, 021113 (2013).

[3]C. J. Docherty, C.-T. Lin, H. J. Joyce, R. J. Nicholas, L. M. Herz, L.-J. Li, and M. B. Johnston, Nat. Commun. **3**, 1228 (2012).

[4]F. Schwierz, Nat. Nanotechnol. **5**, 487 (2010).

[5]J. Li, L. Niu, Z. Zheng, and F. Yan, Adv. Mater. **26**, 5239 (2014).

[6]K. S. Novoselov, V. I. Fal'ko, L. Colombo, P. R. Gellert, M. G. Schwab, and K. Kim, Nature **490**, 192 (2012).

[7]E. W. Hill, A. Vijayaraghavan, and K. Novoselov, IEEE Sens. J. **11**, 3161 (2011).

[8]M. Furchi, A. Urich, A. Pospischil, G. Lilley, K. Unterrainer, H. Detz, P. Klang, A. M. Andrews, W. Schrenk, G. Strasser, and T. Mueller, Nano Lett. **12**, 2773 (2012).

[9]P. Afzali, Y. Abdi, and E. Arzi, J. Nanopart. Res. **16**, 2659 (2014).

[10]K. Kim, J.-Y. Choi, T. Kim, S.-H. Cho, and H.-J. Chung, Nature **479**, 338 (2011).

[11]F. H. L. Koppens, T. Mueller, P. Avouris, A. C. Ferrari, M. S. Vitiello, and M. Polini, Nat. Nanotechnol. **9**, 780 (2014).

[12]L. Vicarelli, M. S. Vitiello, D. Coquillat, A. Lombardo, A. C. Ferrari, W. Knap, M. Polini, V. Pellegrini, and A. Tredicucci, Nat. Mater. **11**, 865 (2012).

[13]X. Cai, A. B. Sushkov, R. J. Suess, M. M. Jadidi, G. S. Jenkins, L. O. Nyakiti, R. L. Myers-Ward, S. Li, J. Yan, D. K. Gaskill, T. E. Murphy, H. D. Drew, and M. S. Fuhrer, Nat. Nanotechnol. **9**, 814 (2014).

[14]P. Avouris and F. Xia, MRS Bull. **37**, 1225 (2012).

[15]B. Chitara, L. S. Panchakarla, S. B. Krupanidhi, and C. N. R. Rao, Adv. Mater. **23**, 5419 (2011).

[16]C. G. Kang, S. K. Lee, T. J. Yoo, W. Park, U. Jung, J. Ahn, and H. B. Lee, Appl. Phys. Lett. **104**, 161902 (2014).

[17]A. Patil, O. Koybasi, G. Lopez, M. Foxe, I. Childres, C. Roecker, J. Boguski, J. Gu, M. L. Bolen, M. A. Capano, I. Jovanovic, P. Ye, and Y. P. Chen, in *IEEE Nuclear Science Symposium and Medical Imaging Conference (NSS/MIC)* (IEEE, 2011), p. 455.

[18]O. Koybasi, E. Cazalas, I. Childres, I. Jovanovic, and Y. P. Chen, in *IEEE Nuclear Science Symposium and Medical Imaging Conference (NSS/MIC)* (IEEE, 2013),p. 1.

[19]P. Docker, J. Kay, and J. Edgeworth, in *TechConnect World- Nanotech: Conference and Expo* (IEEE, 2013).

[20]Y. Liu, R. Cheng, L. Liao, H. Zhou, J. Bai, G. Liu, L. Liu, Y. Huang, and X. Duan, Nat. Commun. **2**, 579 (2011).

[21]D. Sun, G. Aivazian, A. M. Jones, J. S. Ross, W. Yao, D. Cobden, and X. Xu, Nat. Nanotech. **7**, 114 (2012).

[22]M. Freitag, T. Low, and P. Avouris, Nano Lett. **13**, 1644 (2013).

[23]B. Y. Zhang, T. Liu, B. Meng, X. Li, G. Liang, X. Hu, and Q. J. Wang, Nat. Commun. **4**, 1811 (2013).

[24]G. Konstantatos, M. Badioli, L. Gaudreau, J. Osmond, M. Bernechea, F. P. G. de Arquer, F. Gatti, and F. H. L. Koppens, Nat. Nanotechnol. **7**, 363 (2012).

[25]Y. Ren, C. Zhu, W. Cai, H. Li, H. Ji, I. Kholmanov, Y. Wu, R. D. Piner, and R. S. Ruoff, Appl. Phys. Lett. **100**, 163114 (2012).

[26]J. Pezoldt, C. Hummel, and F. Schwierz, Physica E **44**, 985 (2012).

[27]T. J. Echtermeyer, M. C. Lemme, J. Bolten, M. Baus, M. Ramsteiner, and H. Kurz, Eur. Phys. J. Spec. Top. **148**, 19 (2007).

[28]M. Foxe, G. Lopez, I. Childres, R. Jalilian, A. Patil, C. Roecker, J. Boguski, I. Jovanovic, and Y. P. Chen, IEEE Trans. Nanotechnol. **11**, 581 (2012).

[29]D. A. Svintsov, V. V. Vyurkov, V. F. Lukichev, A. A. Orlikovsky, A. Burenkov, and R. Oechsner, Semiconductors **47**, 279 (2013).

[30]Y.-J. Yu, Y. Zhao, S. Ryu, L. E. Brus, K. S. Kim, and P. Kim, Nano Lett. **9**, 3430 (2009).

[31]E. Cazalas, I. Childres, A. Majcher, T.-F. Chung, Y. P. Chen, and I. Jovanovic, Appl. Phys. Lett. **103**, 053123 (2013).

[32]A. Veligura, P. J. Zomer, I. J. Vera-Marun, C. Józsa, P. I. Gordiichuk, and B. J. van Wees, J. Appl. Phys. **110**, 113708 (2011).

[33]J. Meng, H.-C. Wu, J.-J. Chen, F. Lin, Y.-Q. Bie, I. V. Shvets, D.-P. Yu, and Z.-M. Liao, Small **9**, 2240 (2013).

[34]Z.-M. Liao, B.-H. Han, Y.-B. Zhou, and D.-P. Yu, J. Chem. Phys. **133**, 044703 (2010).

[35]B. K. Sarker, I. Childres, E. Cazalas, I. Jovanovic, and Y. P. Chen, preprint arXiv:1409.5725 (2014).

[36]O. Ochedowski, K. Marinov, G. Wilbs, G. Keller, N. Scheuschner, D. Severin, M. Bender, J. Maultzsch, F. J. Tegude, and M. Schleberger, J. Appl. Phys. **113**, 214306 (2013).

[37]I. Childres, L. A. Jauregui, M. Foxe, J. Tian, R. Jalilian, I. Jovanovic, and Y. P. Chen, Appl. Phys. Lett. **97**, 173109 (2010).

[38]A. Sakdinawat and D. Attwood, Nat. Photonics. **4**, 840 (2010).

[39]L. Mihailescu, K. Vetter, M. Burks, E. Hull, and W. Craig, Nucl. Instrum. Methods Phys. Res., Sect. A **570**, 89 (2007).

[40]A. Beyerle, J. P. Hurley, and L. Tunnell, Nucl. Instrum. Methods Phys. Res., Sect. A **299**, 458 (1990).

[41]F. Nava, E. Vittone, P. Vanni, G. Verzellesi, P. Fuochi, C. Lanzieri, and M. Glaser, Nucl. Instrum. Methods Phys. Res., Sect. A **505**, 645 (2003).

[42]A. Kinoshita, M. Iwami, K.-i. Kobayashi, I. Nakano, R. Tanaka, T. Kamiya, A. Ohi, T. Ohshima, and Y. Fukushima, Nucl. Instrum. Methods Phys. Res., Sect. A **541**, 213 (2005).

[43]H. Rabus, V. Persch, and G. Ulm, Appl. Opt. **36**, 5421 (1997).

[44]A. Gottwald, U. Kroth, M. Krumrey, M. Richter, F. Scholze, and G. Ulm, Metrologia **43**, S125 (2006).

[45]M. Krumrey, L. Büermann, M. Hoffmann, P. Müller, F. Scholze, G. Ulm, and T. Warwick, AIP Conf. Proc. **705**, 861 (2004).

[46]S. Nishino, A. J. Powell, and H. A. Will, Appl. Phys. Lett. **42**, 460 (1983).

[47]S. H. Lee, M. Choi, T.-T. Kim, S. Lee, M. Liu, X. Yin, H. K. Choi, S. S. Lee, C.-G. Choi, S.-Y. Choi, X. Zhang, and B. Min, Nat. Mater. **11**, 936 (2012).

[48]D. H. Auston, R. R. Freeman, P. R. Smith, D. M. Mills, and R. H. Siemann, Appl. Phys. Lett. **42**, 1050 (1983).

[49]S. Zou, P. Song, L. Guo, and W. Pei, Rev. Sci. Instrum. **84**, 093508 (2013).

[50]A. P. Artyomov, E. H. Baksht, V. F. Tarasenko, A. V. Fedunin, S. A. Chaikovsky, P. N. Aruev, V. V. Zabrodskii, M. V. Petrenko, N. A. Sobolev, and V. L. Suhanov, Instrum. Exp. Tech **58**, 102 (2015).

[51]S. Kar, A. Vijayaraghavan, C. Soldano, S. Talapatra, R. Vajtai, O. Nalamasu, and P. M. Ajayan, Appl. Phys. Lett. **89**, 132118 (2006).

[52]H. Wang, Y. Wu, C. Cong, J. Shang, and T. Yu, ACS Nano **4**, 7221 (2010).

[53]Y. Paska and H. Haick, ACS Appl. Mater. Interfaces **4**, 2604 (2012).

[54]See supplementary material at http://dx.doi.org/10.1063/1.4921755 for information that discusses (I) methods (II) graphene $I_{sd} - V_g$ measurements (III) effect of gold contacts (IV) calculation of responsivity and time constant (V) gate voltage dependence (VI) mechanism of GFET response, and (VII) model of GFET response.